Change Detection for Synthetic Aperture Radar Images Based on Pattern and Intensity Distinctiveness Analysis

Xiao Wang, Feng Gao, Junyu Dong, Qiang Qi
Ocean University of China, Department of Computer Science and Technology

ABSTRACT

Synthetic aperture radar (SAR) image is independent on atmospheric conditions, and it is the ideal image source for change detection. Existing methods directly analysis all the regions in the speckle noise contaminated difference image. The performance of these methods is easily affected by small noisy regions. In this paper, we proposed a novel change detection framework for saliency-guided change detection based on pattern and intensity distinctiveness analysis. The saliency analysis step can remove small noisy regions, and therefore makes the proposed method more robust to the speckle noise. In the proposed method, the log-ratio operator is first utilized to obtain a difference image (DI). Then, the saliency detection method based on pattern and intensity distinctiveness analysis is utilized to obtain the changed region candidates. Finally, principal component analysis and *k*-means clustering are employed to analysis pixels in the changed region candidates. Thus, the final change map can be obtained by classifying these pixels into changed or unchanged class. The experiment results on two real SAR images datasets have demonstrated the effectiveness of the proposed method.

Keywords: change detection, *k*-means clustering, pattern and intensity distinctiveness, synthetic aperture radar image.

1. INTRODUCTION

Image change detection is a process to identify the differences from two multi-temporal images which are captured from the same geographical area. It has been widely used in numerous fields, such as environmental monitoring [1], hazard assessment of earthquake [2], medical diagnosis [3] and urban sprawl detection [4]. Thus change detection plays an important role in practical applications. Compared with other remote sensing images such as optical images, hyperspectral images and LIDAR images, synthetic aperture radar (SAR) images presents better performance since SAR sensors are independent of weather conditions. Therefore, SAR image is the ideal source to perform change detections. However, with the presence of speckle noise, SAR image change detection encountered more difficulties than optical images.

In recent years, there are many change detection techniques have been proposed. These techniques are generally composed of three steps: preprocessing, difference image (DI) generation and DI analysis. Most researches focus on the DI generation and DI analysis step. In general, the log-ratio operator is the most widely used method for DI generation, since it is robust to speckle noise. In addition, other methods are also proposed to solve the problem of DI generation. In [5], Gao et al. proposed a modified log-ratio operator to generate DI, which is good at detecting changed small targets in multitemporal SAR images. Yavariabdi et al. [6] proposed a novel method to generate DI by using the structural similarity index measure method, which provides combination of the comparisons of luminance, contrast, and structure between two images.Gao et al. [7] proposed a technique based on PCANet for DI analysis. After some reliable samples are selected, PCANet is utilized for changed and unchanged pixels classification. Li et al. [8] proposed a novel change detection method based on Gabor wavelets and hierarchical classifiers. Gong et al. [9] proposed a method by adding the Markov random field (MRF) into the procedure of fuzzy c-means (FCM) clustering, and the method can obtain satisfying results in speckle noise reduction.

Most existing change detection methods use log-ratio operator to generate a DI. We observed that in the DI, the changed regions are usually salient and distinctive. Therefore, if the DI is enhanced by saliency detection method, the change detection performance can be improved. In this paper, we proposed a novel technique based on saliency detection for SAR image change detection. The log-ratio operator is first utilized to generate a DI. Then, pattern and intensity distinctive analysis [10] is employed to obtain the saliency map of the DI. After that, the original DI and the saliency map are fused to obtain an enhance DI. Finally, principal component analysis and k-means clustering (PCAKM) [11] are used to classify pixels in the enhanced DI into changed and unchanged class.

There are two contributions of the proposed method. First, the pattern and intensity distinctive analysis is used to analyze the DI, and the speckle noise in the original DI can be suppressed to some extent. Second, we proposed a novel framework for SAR image change detection. The framework is comprised of DI enhancement and classification by PCAKM. Experimental results on two real SAR image datasets demonstrate the effectiveness of the proposed method.

The remainder of this paper is organized as follows. Section 2 presents the background of SAR image change detection and the motivation of the proposed method. Section 3 introduces the framework of the proposed method in detail. Section 4 shows the experimental results and analysis. Section 5 makes conclusion remarks of the proposed method.

2. PROBLEM AND MOTIVATOIN

SAR images change detection aims to find the difference area from multitemporal SAR images. These multitemporal images are obtained at the same geographical area but at different times. It is a challenging task to detect changes between multitemporal SAR images because of the presence of speckle noise. Therefore, how to suppress the effect of speckle noise becomes a critical issue.

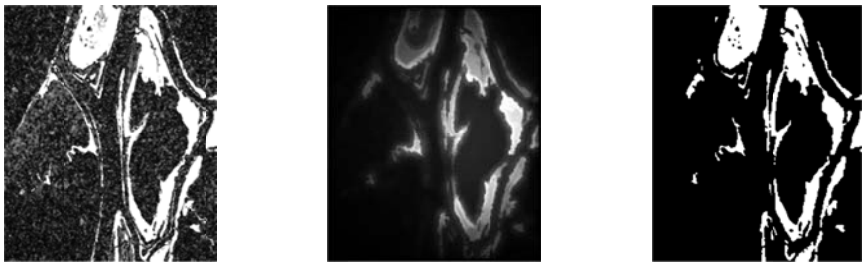

(a) (b) (c)

Figure 1 The similarity between the saliency map and the ground-truth image. (a) Difference image obtained via the log-ratio operator. (b) Saliency map generated by the pattern and intensity distinctiveness analysis [10]. (c) Ground-truth image.

Fig. 1 shows difference image, saliency map and the ground-truth image, respectively. From the difference image, we can observe that the change regions are distinctive and salient. It inspires us to use saliency detection methods to extract these regions. In addition, PCAKM [11] has been proved to be an effective tool in SAR image analysis. Thus, we utilize it to accomplish changed pixels classification.

3. METHODOLOGY

The framework of the proposed method is illustrated in Fig. 2. Specifically, the proposed change detection method is consisted of two steps:

Step 1 — Enhanced DI generation based on pattern and intensity distinctive analysis. The log-ratio operator is first used to generate a DI. Then, pattern and intensity distinctive analysis method [10] is used to generate a saliency map of the DI. The original DI and the saliency map are fused to generate an enhanced DI.

Step2 — Pixels classification via PCAKM. The enhanced DI is partitioned into nonoverlapping blocks. Orthonormal eigenvectors are extracted through principal component analysis (PCA) of these nonoverlapping blocks. Each pixel in the enhanced DI is represented with a feature vector which is the projection of the block data onto the generated eigenvector space. Finally, the feature vectors of all the pixels are classified into changed or unchanged class by using *k*-means clustering.

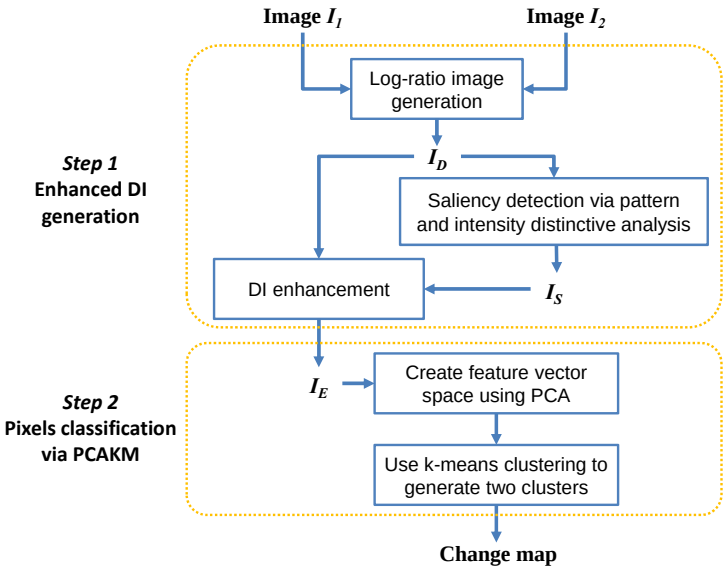

Figure 2 The framework of the proposed method. In the first step, the log-ratio operator is first used to generate a DI, and then the pattern and intensity distinctiveness analysis is utilized to enhance the DI. In the second step, PCAKM [11] is used to classify pixels in the enhanced DI into changed and unchanged clusters.

3.1 Enhanced DI generation based on pattern and intensity distinctive analysis

Given two co-registered multi-temporal SAR images, I_1 and I_2, the log-ratio operator is first used to generate a DI. The log-ratio operator is widely used to handling multitemporal SAR images, since it is considered to be better suited for the intrinsic speckle noise. Let I_D represents the DI, and the formulation of DI can be defined by

$$I_D = |\log(I_1) - \log(I_2)|. \tag{1}$$

After obtaining the log-ratio image, pattern and intensity distinctiveness analysis [10] is utilized to exploit the most salient regions in the DI. It is originally proposed by Margolin [10] to detect salient objects from natural images. The algorithm is comprised of two parts: pattern distinctiveness and intensity distinctiveness. For pattern distinctiveness, all 9×9 patches are extracted and the average patch p_A is computed. An image patch p_x is considered distinct if the patch connecting it to the average patch p_A, along the principle components, is long. Specifically, pattern distinctiveness $D_P(p_x)$ is defined as:

$$D_P(p_x) = \left\| \tilde{p}_x \right\|_1, \tag{2}$$

where $\tilde{p}_x$ is the coordinates of p_x in the PCA coordinate system.

On the other hand, to compute intensity distinctiveness, the input image is segment into regions by using the SLIC superpixels [12]. Then, the intensity distinctiveness of a region r_x is computed by:

$$D_I(r_x) = \sum_{i=1}^{M} \left\| r_x - r_i \right\|_2, \tag{3}$$

where M is the total number of regions. As mentioned above, the saliency algorithm seeks regions that are salient in both pattern and intensity. Therefore, to integrate the pattern and intensity distinctiveness, the saliency map I_{SAL} is computed by

$$I_{SAL} = D_P \cdot D_I. \tag{4}$$

After obtaining the saliency map I_{SAL}, the enhanced difference image I_{DE} is computed by:

$$I_{\mathrm{DE}} = \exp(k \cdot I_{SAL}) \cdot I_D. \tag{5}$$

In practice, we found that the I_{SAL} is of great significance. Therefore, we use an exponential function to emphasize I_{SAL}. In all our experiments, we use $k = 0.1$ as the scaling factor for the exponential. Fig. 3 shows a visual comparison of original difference image I_D, saliency map I_{SAL}, and the enhanced difference image I_{DE}. We can observe that in I_{DE}, changed regions are emphasized, and noisy region are suppressed.

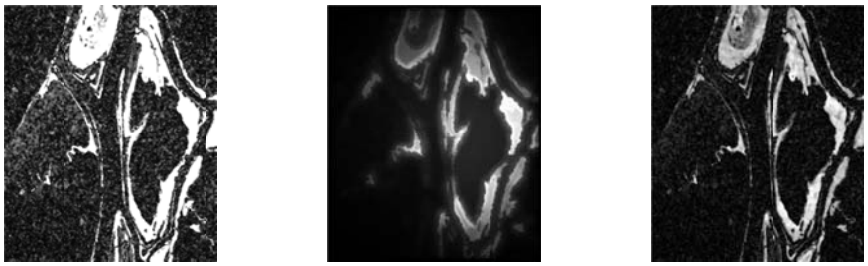

(a) (b) (c)

Figure 3 Illustration of the main phases of DI enhancement. (a) Original DI. (b) Salinecy map obtained by pattern and intensity distinctiveness analysis. (c) Enhanced DI.

3.2 Pixels classification via PCAKM

After obtaining the enhanced difference image I_{DE}, we aim at classifying the pixels in I_{DE} into changed and unchanged class. First, I_{DE} is partitioned into $w \times w$ nonoverlapping blocks. Then, an eigenvector space is created using PCA on these image blocks. Specifically, let $\mathbf{x}^p$ denotes the vector of the pth block, difference vector set Δ_p is computed by $\Delta_p = \mathrm{x}^p - \psi$. Here, ψ represents the average vector of the image block vectors. Next, PCA is applied on the difference vector set Δ_p.

The feature vector space is created by projecting $\mathrm{x}(i,j)$ onto eigenvector space for each pixel at position (i,j), i. e.,

$$\mathbf{v}(i,j) = [v_1, v_2, \cdots v_S]^T, \tag{4}$$

where $1 \le S \le w^2$ and $v_s = \mathbf{e}_s^T(\mathbf{x}(i,j) - \psi)$, $1 \le s \le S$. Here the vector $\mathbf{e}_s$ is the sth eigenvector of the difference vector set Δ_p. The parameter S determines the feature vector $\mathbf{v}(i,j)$, and is the eigenvector used in projecting $\mathbf{x}(i,j)$ onto eigenvector space. In our implementations, the same parameters $w = 4$ and $S = 3$ are used as described in [11].

Next, the feature vector space is clustered by using the *k*-means clustering algorithm, where $k = 2$. After clustering, the average values of both clusters are computed over the DI. Considering that the values of changed pixels are higher than unchanged pixels in the DI. Therefore, the cluster whose pixels have lower average value in the DI is assigned as the unchanged class, and the other cluster is assigned as the changed class.

4. EXPERIMENTS

4.1 Dataset description and experimental settings

In order to evaluate the performance of the proposed method, we use two datasets to accomplish the experimental part. The first dataset is called Bern dataset, which were acquired by the ERS-2 satellite near the city of Bern, Switzerland, in April and May 1999, respectively. During the period between April and May 1999, the River Aare flooded parts of Bern. The changes in the dataset are mainly caused by the flood disaster. The image captured in April 1999 is shown in Fig. 4(a), and the image captured in May 1999 is shown in Fig. 4(b). The ground truth image is shown in Fig. 4(c). It was produced by integrating prior knowledge and photo interpretation.

The second dataset is called the Ottawa dataset, which were acquired by the RADARSAT SAR sensor. Both images were captured in May 1997 and August 1997, respectively. The dataset was provided by the Defense Research and Development, Canada. The changes in the dataset are also caused by flood disaster. The image captured in May 1997 was shown in Fig. 5(a), and the image captured in August 1997 is shown in Fig. 5(b). The ground truth image is shown in Fig. 5(c) which was produced via manual marking by professional interpreters.

The criteria are critical to evaluate the performance of change detection. The criteria used in this paper include false positives (FP), false negatives (FN), overall errors (OE), and percentage correct classification (PCC). FP is the number of

pixels that are unchanged class in the ground truth image but wrongly classified as changed class. FN is the number of pixels that are changed class in the ground truth image but wrongly classified as unchanged class. The OE is the sum of FP and FN. The PCC is computed by $\mathrm{PCC}=(Nu+Nc-\mathrm{FP}-\mathrm{FN})/(Nu+Nc)\times 100\%$, where Nu and Nc denote the actual number of pixels belonging to the unchanged class and changed class, respectively.

The proposed method is compared with PCAKM [11] and GaborTLC [8] in our experiments. Both methods are implemented by using the default parameters provided in the authors' publicly available source codes. In PCAKM [11], $w=4$ and $S=3$ are used. In GaborTLC [8], $V=5$, $k_{\max}=2\pi$, and $U=8$ are used.

4.2 Results on the Bern dataset

Fig. 4 shows the final change maps of different methods on the Bern dataset, and Table 1 lists the criteria of different method for evaluation. In Fig. 4(d) and (e), we can observe that a number of pixels belonging to the unchanged class are falsely classified as the changed class. Therefore, the FP values of PCAKM and GaborTLC are relatively high. By enhancing the DI, the proposed method can effectively suppress the speckle noise. Therefore, the proposed method achieves the minimum FP value and the maximum PCC value. The proposed method obtains better performance than PCAKM and GaborTLC in the Bern dataset.

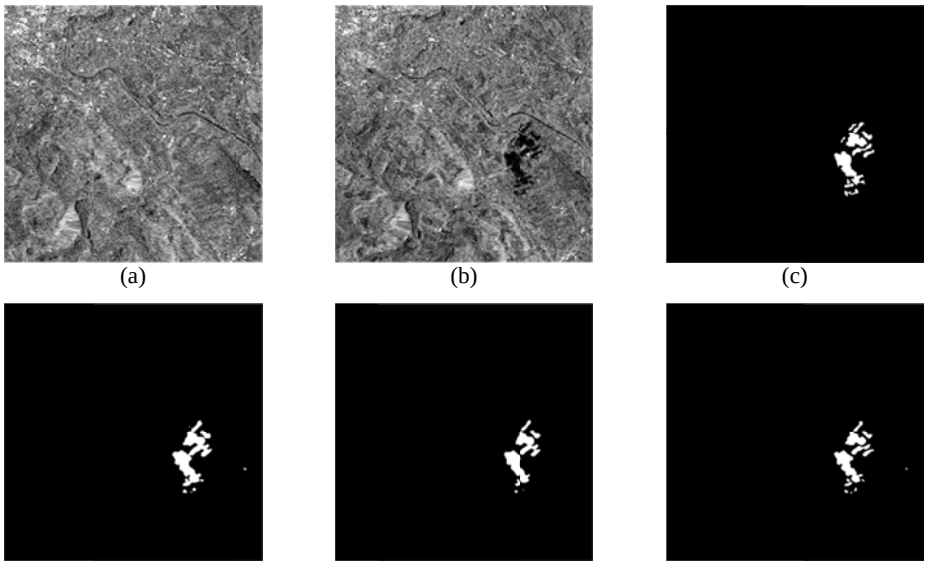

Figure 4. Visualized results of different change detection methods on the Bern dataset. (a) Image captured in April 1999. (b) Image captured in May 1999. (c) Ground truth image. (d) Result by PCAKM. (e) Result by GaborTLC. (f) Result by the proposed method.

Table 1 Change detection results of different methods on the Bern dataset.

Methods	FP	FN	OE	PCC
PCAKM [11]	247	119	366	99.60
GaborTLC [8]	135	173	308	99.66
Proposed method	93	184	277	99.69

4.3 Results on the Ottawa dataset

The visualized results of different methods on the Ottawa dataset are shown in Fig. 5. The evaluation criteria are listed in Table. 2. Similar to the results on the Bern dataset, FP value of the proposed method is the minimum. In addition, from the results generated by PCAKM and GaborTLC, we can observe that some changed pixels are falsely classified into the unchanged class. Therefore, the FN values of these methods are relatively high, and high FN values affect the overall performance of these methods. The proposed method achieves the best OE and PCC values. It demonstrates that the proposed method has good performance in suppressing noisy regions by using pattern and intensity distinctiveness

analysis to neglect some noisy regions. Both visual and quantitative analysis demonstrated the effectiveness of the proposed method.

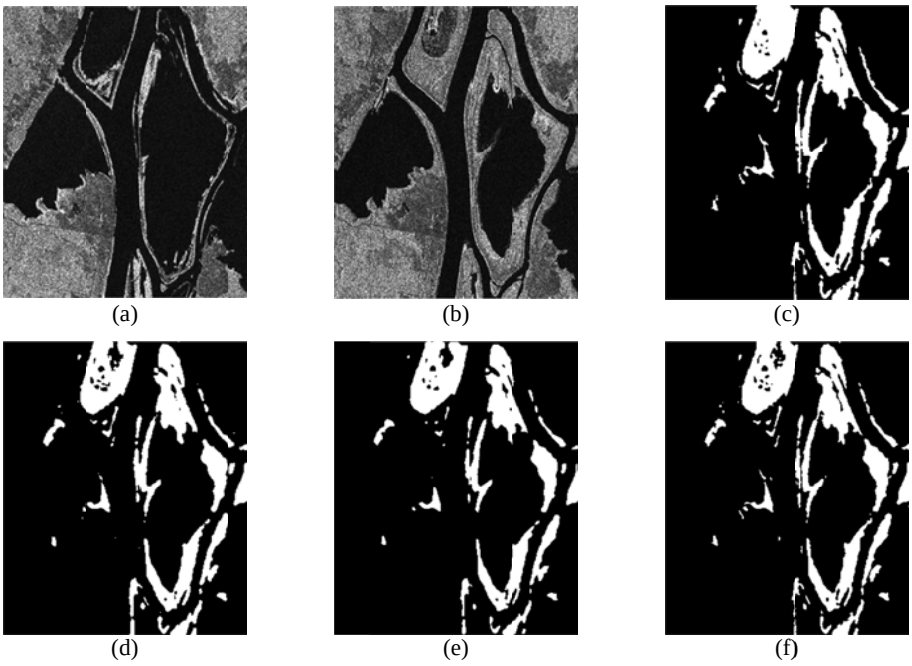

Figure 5. Visualized results of different change detection methods on the Ottawa dataset. (a) Image captured in May 1997. (b) Image captured in August 1997. (c) Ground truth image. (d) Result by PCAKM. (e) Result by GaborTLC. (f) Result by the proposed method.

Table 2 Change detection results of different methods on the Ottawa dataset.

Methods	FP	FN	OE	PCC
PCAKM [11]	955	1515	2470	97.57
GaborTLC [8]	316	1990	2306	97.73
Proposed method	279	1291	1570	98.45

5. CONCLUSION

In this paper, a novel SAR image change detection method based on pattern and intensity distinctiveness analysis is proposed. In the proposed method, the log-ratio operator is first utilized to obtain a difference image. Then, the saliency detection method based on pattern and intensity distinctiveness analysis is utilized to obtain the changed region candidates. Finally, PCAKM method is employed to analyze pixels in the changed region candidates. Thus, final change map can be obtained by classifying these pixels into changed or unchanged class. The experiment results on two real SAR images datasets have demonstrated the effectiveness of the proposed method.

ACKNOELEDGEMENT

The authors would like to thank all the anonymous reviewers for their helpful suggestions. This work was supported by the National Natural Science Foundation of China (No. 41606198, 61271405, 61576011, 61401413) and in part by the Shandong Province Natural Science Foundation of China under Grant ZR2016FB02.

REFERENCES

[1] R. J. Radke, S. Andra and O. Al-Kofahi, "Image change detection algorithms: a systematic survey," *IEEE Trans. Image Process.*, **14**, 294-307, (2005).

[2] R. Nagasawa, "Potential flood hazard assessment by integration of ALOS PALSAR and ASTER GDEM: a case study for the Hoa Chau commune, Hoa Vang district, in central Vietnam," *J. Appl. Remote Sens*., **8**, 083626-083626, (2014).

[3] M. Bosc, F. Heitz, J. P. Armspach, I. Namer, D. Gounot, and L. Rumbach, "Automatic change detection in multimodal serial MRI:application to multiple sclerosis lesion evolution," *Neuroimage*, **20**, 643–656, (2003).

[4] Y. Yang, L. N. Y. Wong and C. Chen, "Using multitemporal Landsat imagery to monitor and model the influences of landscape pattern on urban expansion in a metropolitan region," *J. Appl. Remote Sens.*, **8**, 083639, (2014).

[5] G. Gao, X. Wang and M. Niu, "Modified log-ratio operator for change detection of synthetic aperture radar targets in forest concealment," *J. Appl. Remote Sens.*, **8**, 083583-083583, (2014).

[6] A. Yavariabdi, H. Kusetogullari, "Change Detection in Multispectral Landsat Images Using Multiobjective Evolutionary Algorithm," *IEEE Geosci. Remote Sens. Lett.*, **14**, 414-418, (2017).

[7] F. Gao, J. Dong, B. Li, and Q. Xu, "Automatic Change Detection in Synthetic Aperture Radar Images Based on PCANet," *IEEE Geosci. Remote Sens. Lett.*, **13**,1792-1796, (2016).

[8] H. Li, T. Celik and N. Longbotham, "Gabor feature based unsupervised change detection of multitemporal SAR images based on two-level clustering," *IEEE Geosci. Remote Sens. Lett.*, **12**, 2458-2462, (2015).

[9] M. Gong, L. Su, W. Chen, "Fuzzy clustering with a modified MRF energy function for change detection in synthetic aperture radar images," *IEEE Trans. Fuzzy Syst.*, **22**, 98-109, (2014).

[10] R. Margolin, A. Tal, L. Zelnik-Manor, "What makes a patch distince?" in *2013 IEEE Conference on Computer Vision and Pattern Recognition*, pp. 1139-1146 (2013).

[11] T. Celik, "Unsupervised change detection in satellite images using principal component analysis and k-means clustering," *IEEE Geosci. Remote Sens. Lett.*, **6**, 772-776, (2009).

[12] R. Achanta et al., "SLIC superpixels compared to state-of-the-art superpixel mehtods," *IEEE Trans. Pattern Anal. Machine. Intell.*, **32**, 2274-2282, (2012).